A Journal of the Gesellschaft Deutscher Chemiker

Angewandte International Edition GDCh Chemie

www.angewandte.org

Accepted Article

Title: Simultaneous dual-gene diagnosis of SARS-CoV-2 based on CRISPR/Cas9-mediated lateral flow assay

Authors: Erhu Xiong, Ling Jiang, Tian Tian, Menglu Hu, Huahua Yue, Mengqi Huang, Wei Lin, Yongzhong Jiang, Debin Zhu, and Xiaoming Zhou

This manuscript has been accepted after peer review and appears as an Accepted Article online prior to editing, proofing, and formal publication of the final Version of Record (VoR). This work is currently citable by using the Digital Object Identifier (DOI) given below. The VoR will be published online in Early View as soon as possible and may be different to this Accepted Article as a result of editing. Readers should obtain the VoR from the journal website shown below when it is published to ensure accuracy of information. The authors are responsible for the content of this Accepted Article.

To be cited as: *Angew. Chem. Int. Ed.* 10.1002/anie.202014506

Link to VoR: https://doi.org/10.1002/anie.202014506

WILEY-VCH

10.1002/anie.202014506

RESEARCH ARTICLE

WILEY-VCH

Simultaneous dual-gene diagnosis of SARS-CoV-2 based on CRISPR/Cas9-mediated lateral flow assay

Erhu Xiong[a,b]†, Ling Jiang[b]†, Tian Tian[a], Menglu Hu[a], Huahua Yue[a], Mengqi Huang[a], Wei Lin[a], Yongzhong Jiang[c], Debin Zhu[d], and Xiaoming Zhou*[a]

[a] Dr. Erhu Xiong, Tian Tian, Menglu Hu, Huahua Yue, Mengqi Huang, Wei Lin, Prof. Xiaoming Zhou
School of Life Sciences
South China Normal University
Guangzhou 510631, China
E-mail: zhouxm@scnu.edu.cn

[b] Dr. Ling Jiang
State Key Laboratory of Chemo/Biosensing and Chemometrics, College of Chemistry and Chemical Engineering
Hunan University
Changsha 410082, China

[c] Dr. Yongzhong Jiang
Hubei Provincial Center for Disease Control and Prevention
Wuhan 430079, China

[d] Prof. Debin Zhu
Guangzhou Key Laboratory of Analytical Chemistry for Biomedicine, School of Chemistry
South China Normal University
Guangzhou 510006, China

†These authors contributed equally to this work.

Supporting information for this article is given via a link at the end of the document.

Abstract: Accurate and large-scale screening of infected individuals has proven to be an effective means to control the spread of COVID-19. Currently, many assays have been developed to meet the huge testing requirements and the availability of diverse detection settings. However, few methods emphasize the capability to simultaneously detect two genes in a single test, which is a key measure to improve detection accuracy, as adopted by the gold standard RT-qPCR method. Herein, we developed a CRISPR/Cas9-mediated triple-line lateral flow assay (TL-LFA) combined with multiplex reverse transcription-recombinase polymerase amplification (RT-RPA) for rapid and simultaneous dual-gene detection of SARS-CoV-2 in a single strip test. This assay is characterized by the detection of envelope (E) and open reading frame 1ab (Orf1ab) genes from cell-cultured SARS-CoV-2 and SARS-CoV-2 viral RNA standards, showing a sensitivity of 100 RNA copies per reaction (25 μL). Furthermore, dual-gene analysis of 64 nasopharyngeal swab clinical samples showed 100% negative predictive agreement (NPA) and 97.14% positive predictive agreement (PPA). Expectantly, this developed platform will provide a more accurate and convenient pathway for diagnosis of COVID-19 or other infectious diseases in low-resource regions.

Introduction

Severe acute respiratory syndrome coronavirus 2 (SARS-CoV-2), as an emerging human virus, has caused a serious outbreak of coronavirus disease 2019 (COVID-19) and is threatening the public healthcare systems and human lives around the world.[1–3] To date, due to the lack of effective therapeutics and vaccines for COVID-19, screening as many symptomatic and asymptomatic infected individuals as possible and tracking their contacts is the most effective approach to prevent the spread of the disease.[4–6] At present, detection methods for SARS-CoV-2 are mainly divided into three categories: chest computed tomography (CT), serological test, and nucleic acid test.[7,8] Chest CT is able to detect lung lesion in patients at developed stage of the COVID-19, but it cannot accurately identify the lung changes in mild or asymptomatic patients, and it is also not highly specific for COVID-19 because other viruses or diseases can also cause similar radiologic phenomena.[9–11] Moreover, chest CT cannot be used as a high-throughput screening method due to the risk of cross-infection. Serological tests mainly detect antibodies including IgA, IgG, and IgM in the patient's serum samples. Although serological tests can supply detection result rapidly, it may take several days to weeks for infected individuals to generate detectable antibody response after the onset of symptoms.[12,13] Thus, serological tests are also not suitable as an efficient early diagnosis tool for SARS-CoV-2 infection due to low accuracy. Nucleic acid tests can directly detect SARS-CoV-2 viral RNA extracted from the patient's throat or nasopharyngeal swabs. Recent works have shown that the virus titer in patient's body is very high even in the first few days of SARS-CoV-2 infection,[7,14] which is pivotal for detecting SARS-CoV-2 viral RNA to prevent the infected and asymptomatic individuals from infecting healthy people. Consensus is now solid that nucleic acid tests are more suitable for rapid and sensitive diagnosis of SARS-CoV-2 infection at an early stage to prevent and control the COVID-19 pandemic.

Due to its high sensitivity and specificity, the reverse transcription-real time quantitative polymerase chain reaction (RT-qPCR) is considered as the gold standard method in laboratories and clinical diagnosis for nucleic acid-based SARS-CoV-2 detection.[13,15,16] However, the RT-qPCR method requires specialized and expensive equipment, professional operation, and long turnaround time from sample to result, which is always unrealistic for its use in less-developed countries or resource-limited settings.[17–21] Therefore, it is still essential and meaningful to develop simple, rapid, and field-deployable point-of-care (POC) platforms for SARS-CoV-2 detection that can be used in schools, local clinics, home diagnostics, regional airports, or remote areas with limited instrumental resources.

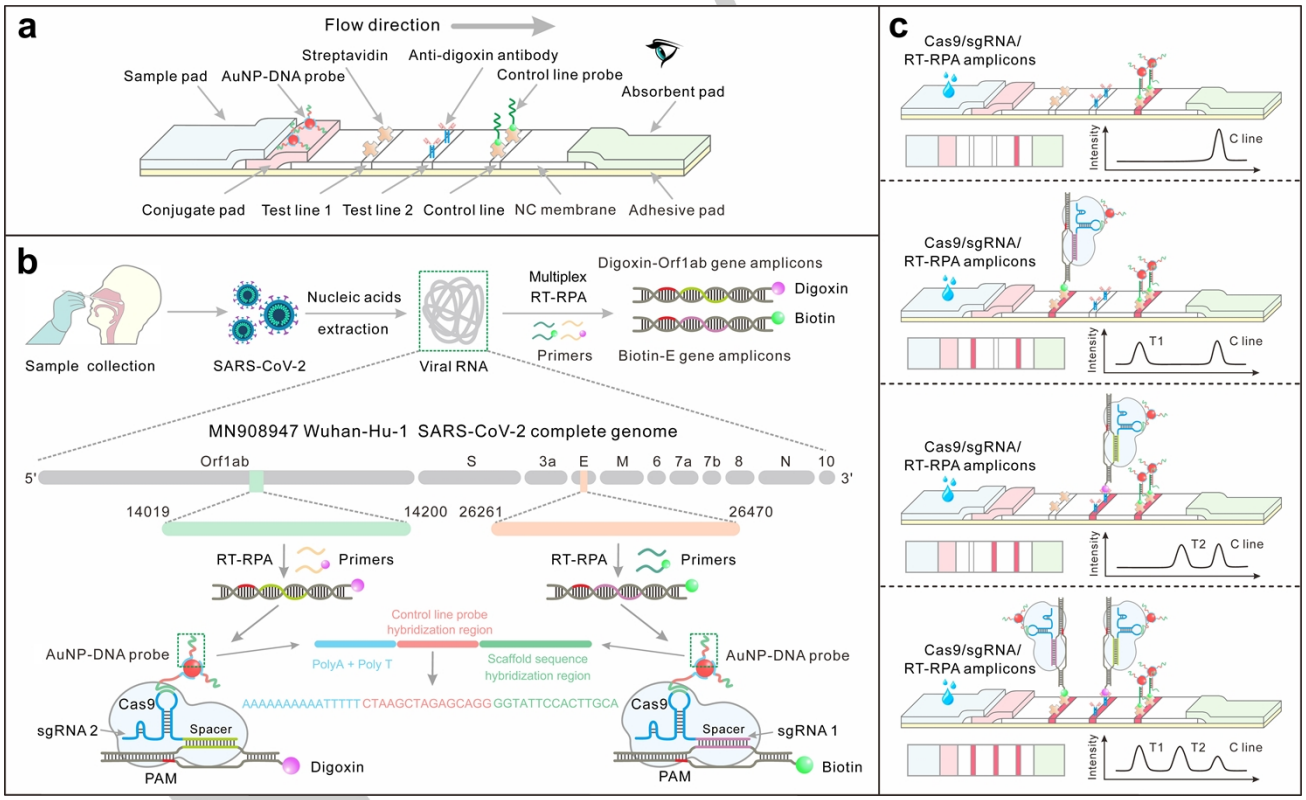
As an effective complement to the RT-qPCR method, various SARS-CoV-2 diagnosis and screening platforms have been developed for better accessibility. Most of these detection

This article is protected by copyright. All rights reserved.

Accepted Manuscript

platforms use isothermal amplification to reduce instrument dependence.[21–30] Some of these methods show improved sensitivity, specificity, and convenience by combining CRISPR technology with fluorescence or test strip detection.[16–18,31–36] Although significant progress has been made, a widely overlooked issue is that most of these methods only demonstrate their application in single-gene analysis.[16–18,21–36] For SARS-CoV-2 diagnosis, reliability is particularly important because false-negative results will cause the actual infected person to be missed, resulting in uncontrollable viral transmission. Simultaneous detection of two genes, as adopted by the clinical approved RT-qPCR method, is usually more accurate than a single-gene test. By employing a dual-gene test, the potential false-negative results caused by partial gene degradation, gene copy number differences, and amplification errors, can be more effectively avoided.[37–39] Therefore, development of POC technology that can detect two genes simultaneously in a single test will be very helpful to improve the detection accuracy, efficiency, and clinical applicability.

The clustered regularly interspaced short palindromic repeats (CRISPR)/Cas system can be integrated into established biosensing platforms [40,41] Recently, our group reported a CRISPR/Cas9-mediated lateral flow assay (CASLFA) for user-friendly gene detection with excellent sensitivity and specificity.[42] In this design, Cas9/sgRNA can be employed for both DNA recognition and bridging of gold nanoparticle (AuNP)-DNA probes. Specifically, the scaffold sequence in the loop region of sgRNA contains a binding site for recruiting AuNP-DNA probes. After the biotinylated amplicons are specifically recognized by Cas9/sgRNA complex, the AuNP-DNA probes will bind to sgRNA and accumulate on the test line. This visible accumulation of AuNP-DNA probes is used for a signal transduction, which can be observed by the naked eye. CASLFA uses Cas9/sgRNA recognition for avoiding tedious nucleic acid hybridization steps and improving specificity, and the test strip detection mode also makes it extremely beneficial to POC applications. However, the original CASLFA version was only designed for single-gene analysis. Herein, we further improved this design and developed a CRISPR/Cas9-mediated triple-line LFA (TL-LFA) combined with multiplex reverse transcription-recombinase polymerase amplification (RT-RPA). A crucial advantage of this platform is the realization of rapid and simultaneous dual-gene detection for SARS-CoV-2 viral RNA. This improved CASLFA is characterized by the detection of envelope (E) and open reading frame 1ab (ORF1ab) genes from cell-cultured SARS-CoV-2 and SARS-CoV-2 viral RNA standards, showing a sensitivity of 100 RNA copies per reaction (25 μL). Furthermore, dual-gene analysis of 64 nasopharyngeal swab clinical samples showed 100% negative predictive agreement (NPA) and 97.14% positive predictive agreement (PPA). Expectantly, this developed platform will provide a more accurate and convenient pathway for diagnosis of SARS-CoV-2 or other infectious diseases in low-resource regions.



Scheme 1. Scheme of the CRISPR/Cas9-mediated TL-LFA. a) Design of the TL-lateral flow strip. The lateral flow strip is composed of sample pad, conjugate pad, absorbent pad, adhesive pad, nitrocellulose filter membrane, test line 1 (T1), test line 2 (T2), and control line (C line). AuNP-DNA probes based on poly adenine (A)-Au conjugation are pre-embedded on the conjugate pad. Streptavidin and anti-digoxin antibodies are pre-embedded on the T1 and T2, respectively. Biotinylated C line probes conjugated with streptavidin are pre-coated on the C line which can hybridize with AuNP-DNA probes. The thick arrow represents the flow direction from sample pad to absorbent pad. b) Brief workflow for multiplex RT-RPA reaction and genome map of SARS-CoV-2 viral RNA showing the amplified region of E gene (from 26261 to 26470) and Orf1ab gene (from 14019 to 14200). Cas9/sgRNA1 and Cas9/sgRNA2 complexes are used for targeting biotin-E gene amplicons and digoxin-Orf1ab gene amplicons, respectively. The universal AuNP-DNA probe includes three functional domains. Poly A + poly T (blue region): Poly A is applied to conjugate with Au and poly T is used as a linker. The green part functions as the binding region with the scaffold sequence in the loop structure of sgRNA. The middle region is used for hybridizing with the precoated biotin-DNA probe on the C line. c) Visual CRISPR/Cas9-mediated TL-LFA readout. Different cases of RT-

This article is protected by copyright. All rights reserved.

Accepted Manuscript

RPA amplicon detection on the TL-lateral flow strips. Four potential test results for TL-lateral flow strips: negative test result, E-gene positive, O-gene positive, and both E-gene and O-gene positive.

Results and Discussion

Scheme of the CRISPR/Cas9-mediated TL-LFA

To achieve the goal of dual-gene detection, we first designed a triple-line lateral flow strip including two test lines (T1 and T2) and a control line (C line) (Scheme 1a). Subsequently, as shown in Scheme 1b, two pairs of specific multiplex RT-RPA primers were designed for E and Orf1ab genes amplification and modified with biotin and digoxin in the forward primers, respectively. The amplified regions are from 26261 to 26470 for E gene and from 14019 to 14200 for Orf1ab gene. We then designed two single-guide RNAs (sgRNA1 and sgRNA2) including a variable recognition sequence (spacer region) and a constant scaffold sequence. Scaffold sequence contains a binding site for recruiting AuNP-DNA probes (Figure S1), and the insertion of scaffold sequence has no significant effect on the binding and cleavage activity of Cas9/sgRNA complex (Figure S2). The designed Cas9/sgRNA1 and Cas9/sgRNA2 complexes could rapidly bind to the biotin-E gene amplicons and Orf1ab gene amplicons via sgRNA programmability. In a typical assay procedure, the above complexes were dropped onto the sample pad, and flowed to the conjugate pad, where the AuNP-DNA probes bound to the scaffold sequence via nucleic acid hybridization. Following hybridization, the complexes were flowed through T1 and T2 successively and were then specifically bound by the pre-coated streptavidin and anti-digoxin antibodies, respectively. Meanwhile, the redundant AuNP-DNA probes flowed through the lateral flow strip and hybridized with the precoated DNA probes on the C line. Finally, the colored bands could be observed by the naked eye due to the AuNPs accumulation (Scheme 1c).

This newly developed dual-target test strip test format will present four potential test results: i. Only C line being visible means a negative test result; ii and iii. Visibility of T1 line and C line or T2 line and C line indicates that only single gene is detected, implying a suspected infection; iv. Both T1 line and T2 line and C line being visible can be used for confirming SARS-CoV-2 infection.

Validation of the CRISPR/Cas9-mediated TL-LFA

To verify the availability of the designed primers for the multiplex RT-RPA reactions, we performed the amplification reaction with the E and Orf1ab gene primers, respectively, in the presence or absence of SARS-CoV-2 viral RNA extracted from the cultured SARS-CoV-2 in Huh 7.5 cells. As shown in Figure 1a, in the presence of SARS-CoV-2 viral RNA, the expected bands for E and Orf1ab gene amplicons could be observed when dual-gene amplification primers were used (Figure 1a, top panel). No amplicon bands appeared in the absence of SARS-CoV-2 viral RNA, thereby validating the RT-RPA reaction specificity. We then investigated the recognition and cleavage capability of Cas9/sgRNA1 and Cas9/sgRNA2 complexes on the E and Orf1ab gene amplicons, respectively, and found in both cases the corresponding Cas9/sgRNA complex exhibited effective cleavage activity (Figure 1a, bottom panel).

Next, we evaluated the recognition specificity of the two designed sgRNAs using strip experiments. As shown in Figure 1b, for sgRNA1, the T1 band appeared on the test strip only in the presence of E gene amplicons, while for sgRNA2, the T2 band could be seen on the test strip only in the presence of Orf1ab gene amplicons, demonstrating no discernible cross-reactivity between the two detection systems. The histogram and heat map analysis of the test line intensity, as analyzed by ImageJ, also exhibited that both sgRNA1 and sgRNA2 had excellent specificities. Therefore, the proposed CRISPR/Cas9-mediated TL-LFA seems can provide a robust diagnostic platform for SARS-CoV-2 viral RNA. Further, we carried out components deletion experiments to confirm the CRISPR/Cas9-mediated TL-LFA concept (Figure 1c). The visual results indicated that this POC platform was only successful in the presence of Cas9 protein, corrected sgRNAs, biotin-E gene/digoxin-Orf1ab gene primers, and SARS-CoV-2 viral RNA. As expected, both T1 and T2 bands could be observed in the presence of both sgRNA1/2 and biotin-E gene/digoxin-Orf1ab gene primers, indicating the feasibility of simultaneous dual-gene detection of SARS-CoV-2 viral RNA combined with multiplex RT-RPA. In this study, Cas9 is adopted for binding-based strip detection because the Cas9/sgRNA complex will not dissociate from the target DNA in a short time after the cleavage reaction is completed.[43-45] Moreover, our experimental results also indicated that the complexes of Cas9/sgRNA/amplicons are stable enough for the detection system and there is no significant difference in analysis efficiency by employing Cas9 and dCas9 proteins (Figure S3).

Accepted Manuscript

This article is protected by copyright. All rights reserved.

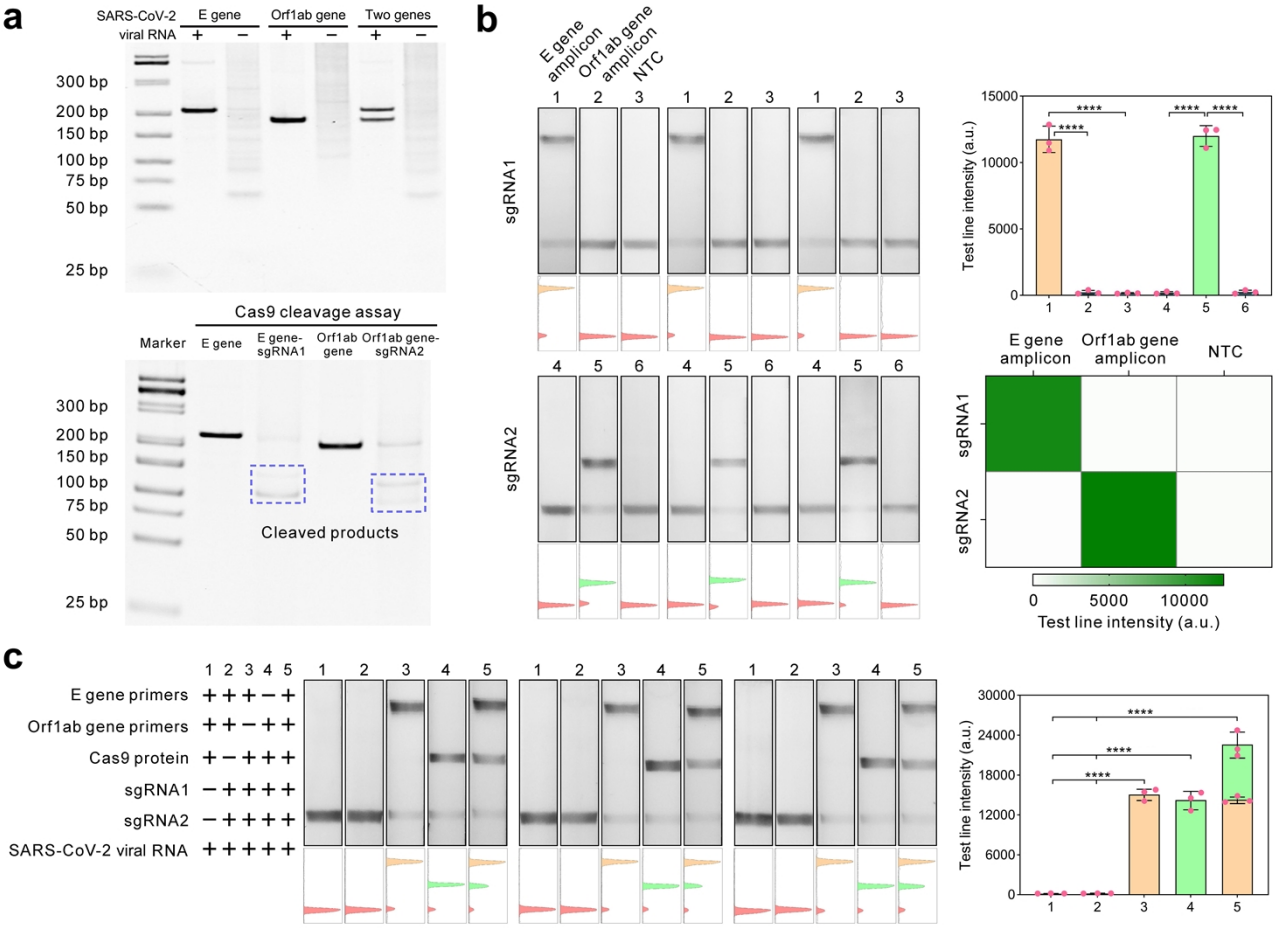


Figure 1. Validation of the CRISPR/Cas9-mediated TL-LFA. a) Top panel: 10% polyacrylamide gel electrophoresis (PAGE) analysis for RT-RPA amplicons of E and Orf1ab genes in the presence/absence of SARS-CoV-2 viral RNA. Bottom panel: 10% PAGE analysis of the CRISPR-Cas9 cleavage assay for E and Orf1ab gene amplicons. Cleaved products (high-temperature denaturation) are shown in the purple dashed boxes. b) Validation of the orthogonal dual-gene detection. The histogram and heat map analysis of the test line intensity as analyzed by ImageJ, show orthogonal detection of E and Orf1ab gene amplicons. c) Components deletion experiments for confirming the CRISPR/Cas9-mediated TL-LFA concept. The histogram represents the value of the test line intensity as analyzed by ImageJ. (n = 3 technical replicates, two-tailed Student's t test; NTC, no template control; *, $p < 0.05$; **, $p < 0.01$; ***, $p < 0.001$; and ****, $p < 0.0001$; error bars represent means ± SD).

Evaluation of analytical performance of the CRISPR/Cas9-mediated TL-LFA

Following the validation of the CRISPR/Cas9-mediated TL-LFA concept, we moved to evaluate the analytical sensitivity and specificity of the detection system. First, we employed the SARS-CoV-2 viral RNA standards which include full-length E and Orf1ab genes to investigate the analytical sensitivity (Figure 2a). SARS-CoV-2 viral RNA standards were obtained by *in vitro* transcription and quantified by droplet digital PCR. After the RT-RPA reactions, the E gene amplicons were subjected to the CRISPR/Cas9 recognition, and the experimental results could be observed visually from T1 bands on the lateral flow strips (Figure 2b). Based on the naked-eye observation or ImageJ grayscale analysis, a limit of detection (LOD) of as low as 100 copies per reaction (25 µL) was obtained for both genes test (Figure 2c).

Subsequently, we assessed the specificity of the proposed CRISPR/Cas9-mediated TL-LFA by using other related coronaviruses including SARS-CoV and bat SARS-like coronavirus (bat-SL-CoVZC45) for E and Orf1ab detection. Due to the extreme high sequence similarity in the amplified region of E gene for all of three coronaviruses, it is impossible for specific detection of SARS-CoV-2 at this target region with our TL-LFA method (Figure S4). Despite this, this region can be considered as a universal target for detecting SARS-CoV-2, SARS-CoV, and bat-SL-CoVZC45. Next, we moved to employ the Orf1ab gene for specificity evaluation. It is anticipated that TL-LFA would show a negative result even if in the presence of other coronaviruses with high sequence homology. This is because a positive detection signal will be ensured by the occurrence of the following events: the correct recognition of target DNA by the RPA primer pairs, protospacer adjacent motif (PAM) site-mediated CRISPR/Cas9 recognition, and complementary pairing between sgRNA and target DNA. As expected, we observed T2 bands only in the presence of SARS-CoV-2 viral RNA, verifying a satisfied specificity for Orf1ab gene (Figure 2d). Our results therefore demonstrated that combining RT-RPA amplification step and the CRISPR/Cas9 detection step can supply reliable SARS-CoV-2 detection (Figure 2d and Figure S5).

This article is protected by copyright. All rights reserved.

Accepted Manuscript

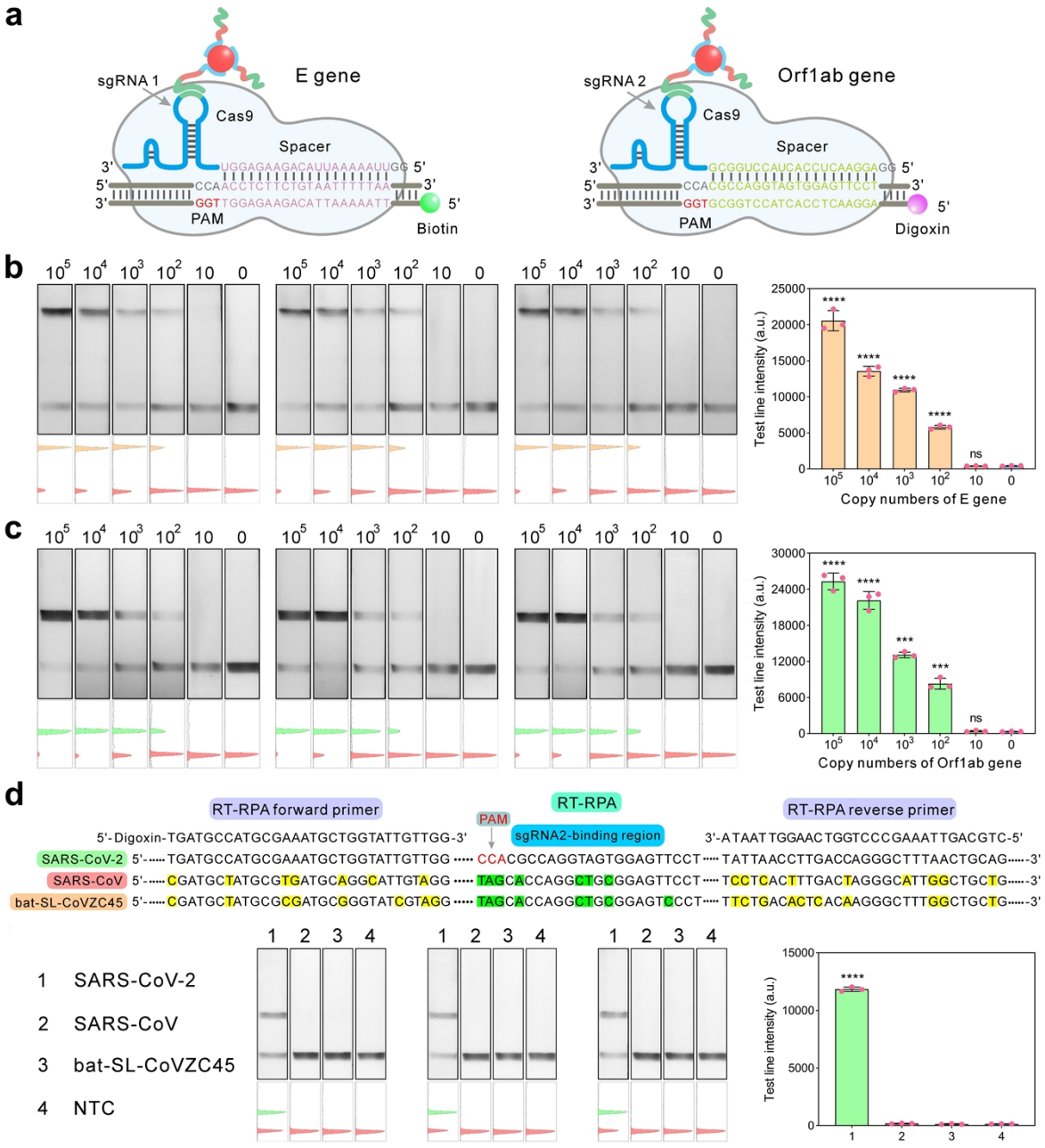


Figure 2. Evaluation of analytical performance of the CRISPR/Cas9-mediated TL-LFA. a) The Cas9/sgRNA-recognized sequences of E and Orf1ab gene amplicons. b) Evaluation of sensitivity of E gene analysis with varied RNA copies. The histogram represents the quantification of the T1 line intensity as analyzed by ImageJ. c) Evaluation of sensitivity of Orf1ab gene analysis with varied RNA copies. The histogram represents the quantification of the T2 line intensity as analyzed by ImageJ. d) Evaluation of analytical specificity of Orf1ab gene. Top panel: Comparison of Orf1ab gene sequences between SARS-CoV-2 (accession MN908947), SARS-CoV (accession NC_004718), and bat-SL-CoVZC45 (accession MG772933) at the sites targeted by RT-RPA primers and sgRNA2. The mismatched bases in the binding region of primers and sgRNA2 are highlighted in yellow and green, respectively. Lower panel: Lateral flow assay using Cas9/sgRNA2 for Orf1ab gene of SARS-CoV-2, SARS-CoV, and bat-SL-CoVZC45. The histogram represents the value of the test line intensity as analyzed by ImageJ. (n = 3 technical replicates, two-tailed Student's t test; NTC, no template control; ns, not significant; *, $p < 0.05$; **, $p < 0.01$; ***, $p < 0.001$; and ****, $p < 0.0001$; error bars represent means ± SD).

Detection of SARS-CoV-2 from nasopharyngeal swab clinical samples

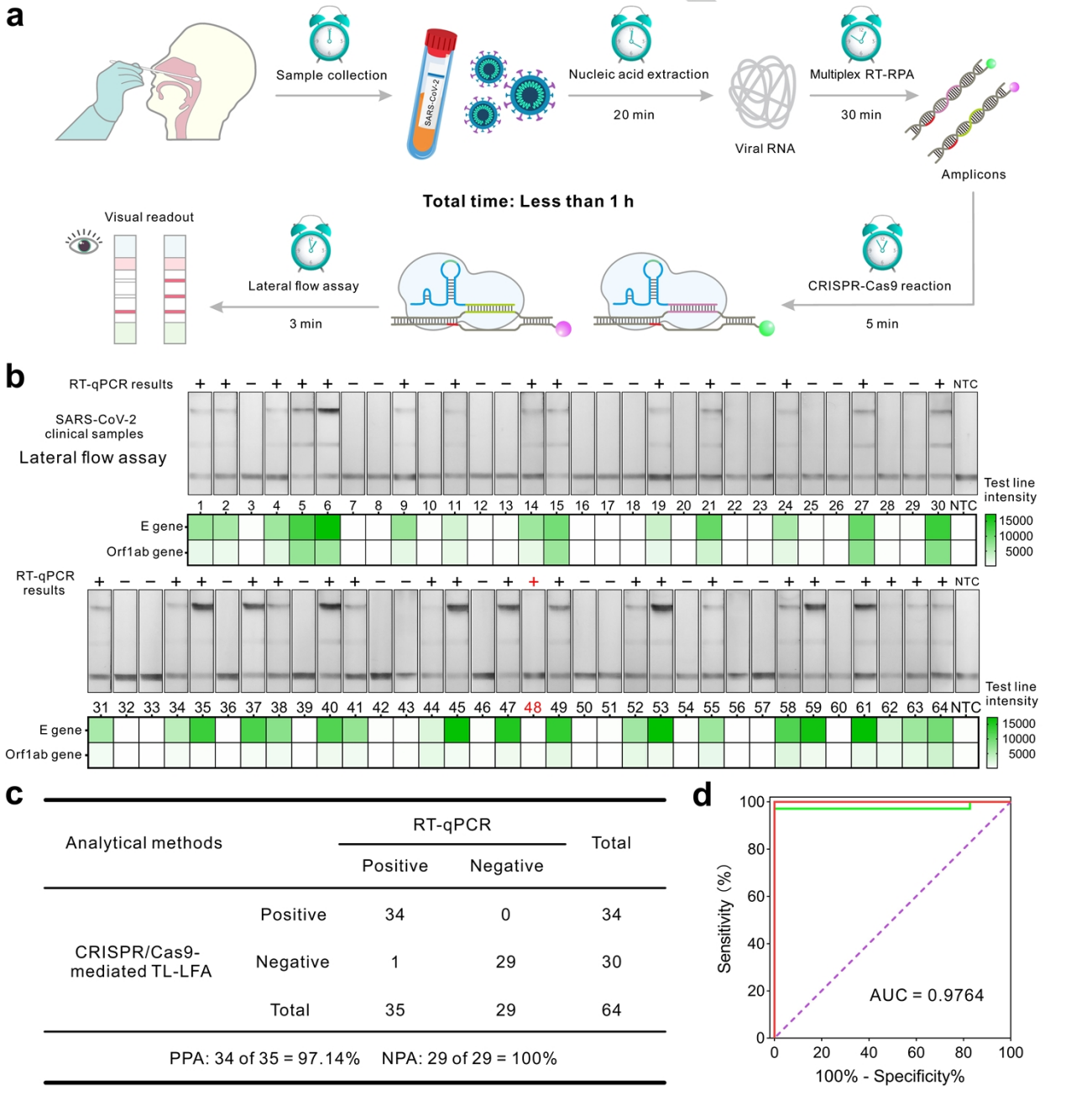
Finally, we validated the practicability of the CRISPR/Cas9-mediated TL-LFA for SARS-CoV-2 detection from a total of 64 nasopharyngeal swab clinical samples consisting of 35 RT-qPCR-confirmed positive samples and 29 RT-qPCR-confirmed negative samples (Figure S6). As shown in Figure 3a, by calculating the time spent in the entire workflow, we have reached a conclusion that CRISPR/Cas9-mediated TL-LFA strategy allow a rapid turnaround time (<1 h) for completing SARS-CoV-2 detection.

As shown in Figure 3b and c, among the 64 nasopharyngeal swab clinical samples, our assay results matched all 29 negative

This article is protected by copyright. All rights reserved.

Accepted Manuscript

COVID-19 samples (100% negative predictive agreement, NPA) and 34 of 35 positive COVID-19 samples (97.14% positive predictive agreement, PPA) with an area-under-the-curve (AUC) value of 0.9764 in the receiver operating characteristic (ROC) curve (Figure 3d), demonstrating excellent sensitivity and specificity. One positive sample (Number 48) was falsely classified as negative in the CRISPR/Cas9-mediated TL-LFA detection. RT-qPCR result showed that this sample has a high cycle threshold (Ct) value of 36.87, implying that the detection of clinical samples at higher Ct values using the TL-LFA method was less robust (Figure S6). However, reliable detection results can be achieved for analyzing clinical samples at lower Ct values (<35). Despite this, the level of sensitivity may be enough for SARS-CoV-2 screening. Some clinical studies have shown that when Ct values are equal to or higher than 34 or the viral load drops below 10^3 copies/μL, the infectivity and the viral transmission risk is low.[46] Recent modeling of viral dynamics also indicated that a LOD of 10^2 copies/μL is qualified for screening of SARS-CoV-2 infection.[14,47,48] It is also worth noting that the test efficiency of Orf1ab gene is lower than that of E gene due to the competition of T1, T2 and C line for AuNP-DNA probes, which may lead to false-negative results. Hence, several potential technical improvements can be performed to the current design in the future. For example, optimizing the number of pre-embedded AuNP-DNA probes to promote sufficient AuNP-DNA probes for signal display on the two test lines, designing two types of AuNP-DNA probes for the identification of each target gene amplicons to avoid the problem of competitive hybridization, or detecting the two gene amplicons separately on the same test line to ensure the recognition of them in a parallel orientation. Additionally, the flow rate of the test strip can be also regulated through optimizing the pore size of the nitrocellulose membrane or the running buffer to ensure better binding efficiency.



This article is protected by copyright. All rights reserved.

Accepted Manuscript

Figure 3. Detection of SARS-CoV-2 in nasopharyngeal swab clinical samples. a) Workflow and time requirements for clinical diagnosis of SARS-CoV-2 using the POC platform. After sample collection, a rapid viral RNA extraction was performed (20 min), followed by the multiplex RT-RPA reaction at 37 °C (30 min), the CRISPR-Cas9 reaction (5 min), and the lateral flow assay (3 min). b) Clinical sample detection by the CRISPR/Cas9-mediated TL-LFA and identification by RT-qPCR. The heat map represents the values of the test line intensity as analyzed by ImageJ. The "+" and "−" represent positive and negative samples, respectively, as confirmed by RT-qPCR. c) Statistical comparison between the CRISPR/Cas9-mediated TL-LFA and RT-qPCR of clinical samples. PPA, positive predictive agreement; NPA, negative predictive agreement. d) ROC curve analysis of the CRISPR/Cas9-mediated TL-LFA detection accuracy in practical applications.

Conclusion

COVID-19 caused by SARS-CoV-2 has spread to almost all countries and regions in the world. Rapid and accurate screening is extremely important to control the continued spread of SARS-CoV-2. Currently almost all SARS-CoV-2 screening and diagnosis task rely on RT-qPCR technology in the laboratory. One way to solve this high-load test task is to develop more user-friendly test technique, which can be used in non-professional laboratory environments even in-home test. Efforts to achieve this goal have led to the development of many new diagnostic methods with POC potential. By adopting isothermal amplification, CRISPR technology, and new user-friendly readout, these methods show more merits, such as lower instrument dependence, faster speed, and better specificity, when compared with the gold standard RT-qPCR method. However, in most of these methods only single-gene testing version is developed.

Single-gene testing may produce false-negative results due to differences in gene copy number, partial RNA degradation, amplification errors, etc. The potential single-gene testing caused false-negative issue can be well resolved by dual-gene testing, a widely adopted strategy by clinical approved RT-qPCR diagnostic kits. Simultaneous dual-gene testing can be easily achieved by optical detection methods with multi-color fluorescent probes.[21,49] However, simultaneous dual-gene testing is very difficult to achieve for many POC-based technologies. For example, some isothermal amplification-based SARS-CoV-2 detection methods, like LAMP, realize visual detection through nonspecific detection of pH change caused by released pyrophosphate ions during the amplification process. However, the color change of the pH indicator will not be able to distinguish which gene has been amplified at a single-tube test. Other POC-based SARS-CoV-2 detection technologies are realized by combining isothermal amplification, such as LAMP and RPA, with CRISPR/Cas12 or CRISPR/Cas13 system. All these methods are based on the detection of target-triggered non-specific *trans*-cleavage of CRISPR/12 and CRISPR/Cas13 system, so multiple detection is also difficult to realize.

In this work, we aim to develop a SARS-CoV-2 detection method to achieve a trade-off between sensitivity, specificity, POC potential, and accuracy. We thus proposed a POC platform for rapid and simultaneous dual-gene detection of SARS-CoV-2 based on the CRISPR/Cas9-mediated TL-LFA combined with multiplex RT-RPA reaction. The realization of dual-gene detection of SARS-CoV-2 viral RNA in a single lateral flow strip test can greatly improve detection accuracy and efficiency. Moreover, unlike RT-qPCR methods, however, our POC platform can be performed in a completely isothermal process (37 °C) without the need of temperature cycling or complex instruments (Figure S7). Next, the assay procedure can be accomplished within 1 h including the viral RNA extraction step, achieving rapid, visual, and sensitive detection with a LOD of 100 copies per reaction (25 μL). Furthermore, by employing Cas9/sgRNA complexes for secondary recognition that effectively eliminate the interference of primer dimers thus improve the specificity. Finally, analysis of 64 nasopharyngeal swab clinical samples showed that the CRISPR/Cas9-mediated TL-LFA method has comparable analytical specificity and sensitivity with the gold-standard RT-qPCR method.

In general, the developed platform can significantly improve the accessibility of diagnostic methods for SARS-CoV-2 infection and provide a potential crucial tool in the fight against the COVID-19 pandemic. Moreover, beyond the COVID-19, the novel integrated POC platform also holds great promise in the surveillance and control of other infectious diseases, especially in resource-limited settings.

Acknowledgements

This work was supported by the National Natural Science Foundation of China (Grants 91959128; 21874049; 21904042; 81772246), the Guangdong Province Science and Technology Plan of (2017B020207011). the Special Support Program of Guangdong Province (Grant 2016TQ03R749), the Opening Project of State Key Laboratory of Chemo/Biosensing and Chemometrics of Hunan University (Grant 2019004) and Open Funds of the State Key Laboratory of Electroanalytical Chemistry (SKLEAC202001). We thank Siyuan (Stella) Wang from the University of Texas at Austin for helpful discussion and revision in the preparation of this manuscript.

Keywords: CRISPR/Cas system • SARS-CoV-2 • lateral flow assay • point-of-care • dual-gene detection

[1] I. Schröder, ACS Chem. *Health Saf.* **2020**, *27*, 160−169.
[2] D. Ivanov, Transp. Res. E Logist. *Transp. Rev.* **2020**, *136*, 101922−101936.
[3] L. Q. Xia, *Acta Laser Biology Sinica* **2020**, *29*, 1−10.
[4] C. J. Wang, C. Y. Ng, R. H. Brook, *JAMA* **2020**, *323*, 1341–1342.
[5] M. Salathé, C. Althaus, R. Neher, S. Stringhini, E. Hodcroft, J. Fellay, M. Zwahlen, G. Senti, M. Battegay, A. Wilder-Smith, et al., *Swiss Med. Wkly.* **2020**, *150*, w202205.
[6] L. Ferretti, C. Wymant, M. Kendall, L. L. Zhao, A. Nurtay, L. Abeler-Dörner, M. Parker, D. Bonsall, C. Fraser, Science 2020, 368, eabb6936.
[7] M. N. Esbin, O. N. Whitney, S. S. Chong, A. Maurer, X. Darzacq, R. Tjian, *RNA* **2020**, doi:10.1261/rna.076232.120.
[8] Y. H. Xu, J. H. Dong, W. M. An, X. Y. Lv, X. P. Yin, J. Z. Zhang, D. Li, H. J. Zhang, B. L. Gao, *J. Infection* **2020**, 80, 394−400.
[9] X. Xu, C. C. Yu, J. Qu, L. G. Zhang, S. F. Jiang, D. Y. Huang, B. H. Chen, Z. P. Zhang, W. H. Guan, Z. K. Ling, et al., *Eur. J. Nucl. Med. Mol. I.* **2020**, *47*, 1275−1280.
[10] M. Schiller, S. Wydra, H. U. Kerl, W. Kick, *J. Med. Virol.* **2020**, *92*, 2863−2865.
[11] H. X. Bai, R. B. Wang, Z. Xiong, B. Hsieh, K. Chang, K. Halsey, X. L. Jiang, I. Pan, Q. H. Zeng, P. F. Hu, et al., *Radiology* **2020**, *296*, E156−E165.

This article is protected by copyright. All rights reserved.

Accepted Manuscript

[12] W. Zhang, R. H. Du, B. Li, X. S. Zheng, X. L. Yang, B. Hu, Y. Y. Wang, G. F. Xiao, B. Yan, Z. L. Shi, et al., *Emerg. Microbes Infect.* **2020**, *9*, 386–389.

[13] B. Udugama, P. Kadhiresan, H. N. Kozlowski, A. Malekjahani, M. Osborne, V. Y. C. Li, H. Chen, S. Mubareka, J. B. Gubbay, W. C. W. Chan, *ACS Nano* **2020**, *14*, 3822–3835.

[14] R. Wölfel, V. M. Corman, W. Guggemos, M. Seilmaier, S. Zange, M. A. Müller, D. Niemeyer, T. C. Jones, P. Vollmar, C. Rothe, et al., *Nature* **2020**, *581*, 465–469.

[15] C. B. F. Vogels, A. F. Brito, A. L. Wyllie, J. R. Fauver, I. M. Ott, C. C. Kalinich, M. E. Petrone, A. Casanovas-Massana, M. C. Muenker, A. J. Moore, et al., *Nat. Microbiol.* **2020**, *5*, 1299–1305.

[16] M. Patchsung, K. Jantarug, A. Pattama, K. Aphicho, S. Suraritdechachai, P. Meesawat, K. Sappakhaw, N. Leelahakorn, T. Ruenkam, T. Wongsatit, et al., *Nat. Biomed. Eng.* **2020**, doi:10.1038/s41551-020-00603-x.

[17] J. P. Broughton, X. D. Deng, G. H. Yu, C. L. Fasching, V. Servellita, J. Singh, X. Miao, J. A. Streithorst, A. Granados, A. Gonzalez-Sotomayor, et al., *Nat. Biotechnol.* **2020**, *38*, 870–874.

[18] X. J. Wang, M. T. Zhong, Y. Liu, P. X. Ma, L. Dang, Q. Z. Meng, W. W. Wan, X. D. Ma, J. Liu, G. Yang, et al., Sci. Bull. 65, 1436–1439 (2020).

[19] A. M. Butt, S. Siddique, X. P. An, Y. G. Tong, *medRxiv* **2020**, doi:10.1101/2020.04.08.20056986.

[20] A. Niemz, T. M. Ferguson, D. S. Boyle, *Trends Biotechnol.* **2011**, *29*, 240–250.

[21] C. H. Woo, S. Jang, G. Shin, G. Y. Jung, J. W. Lee, *Nat. Biomed. Eng.* **2020**, doi:10.1038/s41551-020-00617-5.

[22] V. L. D. Thi, K. Herbst, K. Boerner, M. Meurer, L. P. Kremer, D. Kirrmaier, A. Freistaedter, D. Papagiannidis, C. Galmozzi, M. L. Stanifer, et al., *Sci. Transl. Med.* **2020**, *12*, eabc7075.

[23] B. A. Rabe, C. Cepko, *Proc. Natl. Acad. Sci. USA* **2020**, *117*, 24450–24458.

[24] M. A. Crone, M. Priestman, M. Ciechonska, K. Jensen, D. J. Sharp, A. Anand, P. Randell, M. Storch, P. S. Freemont, *Nat. Commun.* **2020**, *11*, 4464.

[25] J. Jiao, C. J. Duan, L. Xue, Y. F. Liu, W. H. Sun, Y. Xiang, *Biosens. Bioelectron.* **2020**, *167*, 112479.

[26] B. Tian, F. Gao, J. Fock, M. Dufva, M. F. Hansen, *Biosens. Bioelectron.* **2020**, *165*, 112356.

[27] A. Ganguli, A. Mostafa, J. Berger, M. Y. Aydin, F. Sun, S. A. Stewart de Ramirez, E. Valera, B. T. Cunningham, W. P. King, *Proc. Natl. Acad. Sci. USA* **2020**, *117*, 22727–22735.

[28] B. Schermer, F. Fabretti, M. Damagnez, V. D. Cristanziano, E. Heger, S. Arjune, N. A. Tanner, T. Imhof, M. Koch, A. Ladha, et al., *PLoS One* **2020**, doi:10.1371/journal.pone.0238612.

[29] S. Bhadra, T. E. Riedel, S. Lakhotia, N. D. Tran, A. D. Ellington, *bioRxiv* **2020**, doi:10.1101/2020.04.13.039941.

[30] Q. X. Wu, C. Q. Suo, T. Brown, T. Wang, T. Y. Wang, S. A. Teichmann, A. R. Bassett, *bioRxiv* **2020**, doi:10.1101/2020.06.01.127019.

[31] X. Ding, K. Yin, Z. Y. Li, R. V. Lalla, E. Ballesteros, M. M. Sfeir, C. C. Liu, *Nat. Commun.* **2020**, *11*, 4711.

[32] P. X. Ma, Q. Z. Meng, B. Q. Sun, B. Zhao, L. Dang, M. T. Zhong, S. Y. Liu, H. T. Xu, H. Mei, J. Liu, et al., *Adv. Sci.* **2020**, 2001300.

[33] D. Huang J. J. Qian, Z. W. Shi, J. R. Zhao, M. J. Fang, Z. N. Xu, *ACS Synth. Biol.* **2020**, *9*, 3114–3123.

[34] Y. J. Chen, Y. Shi, Y. Chen, Z. N. Yang, H. Wu, Z. H. Zhou, J. Li, J. F. Ping, L. P. He, H. Shen, et al., *Biosens. Bioelectron.* **2020**, *169*, 112642.

[35] L. Guo, X. H. Sun, X. G. Wang, C. Liang, H. P. Jiang, Q. Q. Gao, M. Y. Dai, B. Qu, S. Fang, Y. H. Mao, et al., *Cell Discov.* **2020**, *6*, 34.

[36] J. Arizti-Sanz, C. A. Freije, A. C. Stanton, C. K. Boehm, B. A. Petros, S. Siddiqui, B. M. Shaw, G. Adams, T. F. Kosoko-Thoroddsen, M. E. Kemball, et al., *Nat. Commun.* **2020**, 11, 5921.

[37] P. Trémeaux, S. Lhomme, F. Abravanel, S. Raymond, C. Mengelle, J. M. Mansuy, J. Izopet, *J. Clin. Virol.* **2020**, *129*, 104541.

[38] M. Wang, A. S. Fu, B. Hu, Y. Q. Tong, R. Liu, Z. Liu, J. S. Gu, B. Xiang, J. H. Liu, W. Jiang, et al., *Small* **2020**, *16*, 2002169.

[39] D. Kim, Y. Y. Lee, J. S. Yang, J. W. Kim, V. N. Kim, H. Chang, *Cell* **2020**, *181*, 914−921.

[40] Y. F. Dai, Y. F. Wu, G. Z. Liu, J. J. Gooding, *Angew. Chem.* **2020**, *132*, 2–15.

[41] W. Xu, T. Jin, Y. Dai, C. C. Liu, *Biosens. Bioelectron.* **2020**, *155*, 112100.

[42] X. S. Wang, E. H. Xiong, T. Tian, M. Cheng, W. Lin, H. Wang, G. H. Zhang, J. Sun, X. M. Zhou, *ACS Nano* **2020**, *14*, 2497−2508.

[43] C. D. Richardson, G. J. Ray, M. A. DeWitt, G. L. Curie, J. E. Corn, *Nat. Biotechnol.* **2016**, *34*, 339−344.

[44] A. T. Raper, A. A. Stephenson, Z. Suo, *J. Am. Chem. Soc.* **2018**, *140*, 2971−2984.

[45] S. H. Sternberg, S. Redding, M. Jinek, E. C. Greene, J. A. Doudna, *Nature* **2014**, *507*, 62−67.

[46] D. B. Larremore, B. Wilder, E. Lester, S. Shehata, J. M. Burke, J. A. Hay, M. Tambe, M. J. Mina, R. Parker, *medRxiv* **2020**, doi:10.1101/2020.06.22.20136309.

[47] K. Quicke, E. Gallichotte, N. Sexton, M. Young, A. Janich, G. Gregory, E. J. Carlton, N. Ehrhart, G. D. Ebel, *medRxiv* **2020**, doi:10.1101/2020.06.08.20125989.

[48] B. L. Scola, M. L. Bideau, J. Andreani, V. T. Hoang, C. Grimaldier, P. Colson, P. Gautret, D. Raoult, *Eur. J. Clin. Microbiol. Infect. Dis.* **2020**, *39*, 1059−1061.

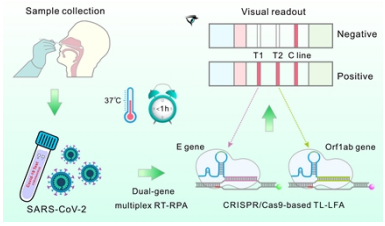
[49] S. M. Xia, X. Chen, *Cell Discov.* **2020**, *6*, 37.

This article is protected by copyright. All rights reserved.

Accepted Manuscript

10.1002/anie.202014506

Entry for the Table of Contents



A CRISPR/Cas9-mediated triple-line lateral flow assay was developed combining with multiplex reverse transcription-recombinase polymerase amplification (RT-RPA) for simultaneous dual-gene diagnosis of SARS-CoV-2. With this platform, the cell-cultured SARS-CoV-2, SARS-CoV-2 viral RNA standards, and nasopharyngeal swab clinical samples could be sensitively and specifically detected.

WILEY-VCH
Accepted Manuscript

This article is protected by copyright. All rights reserved.